Hyperfine Interactions
https://doi.org/10.1007/s10751-019-1558-y

A novel hybrid nanoparticle based on Fe_3O_4/TMAOH/poly(L-co-D,L lactic acid-co-trimethylene carbonate) prepared through the solvent displacement method

Vagner de Oliveira Machado[1] · Ângela Leão Andrade[2] · Luis Carlos Duarte Cavalcante[3,4] · José Domingos Fabris[4,5] · Rosana Zacarias Domingues[4] · José Domingos Ardisson[6] · Luís E. Fernandez-Outon[6] · Carmen Pizarro[7] · Carlos Nelson Elias[1]

Published online: 11 March 2019

Abstract
TMAOH-dispersed nanoparticles of magnetite were first prepared through the reduction–precipitation of ferric chloride with Na_2SO_3 and NH_4OH. The TMAOH-dispersed (Fe_3O_4) magnetic nanoparticles were then surface-coated with poly(L-co-D,L lactic acid-co-trimethylene carbonate) (PLDLA-co-TMC) to obtain the corresponding hybrid system (Fe_3O_4/TMAOH/PLDLA-co-TMC). Samples of so prepared material were analyzed by Fourier-transform infrared spectroscopy (FTIR), powder X-ray diffraction (XRD), magnetization measurements up to 2.5 T, and Mössbauer spectroscopy. Results indicate that this magnetic iron oxide soon after the synthesis is structurally close enough to a typically pure stoichiometric magnetite. FTIR data support clears evidences confirming the efficiency of the solvent displacement method to assure coating the TMAOH-dispersed (Fe_3O_4) magnetic nanoparticles with the terpolymer while preserves the main chemical structural characteristic of the nanosized magnetite.

Keywords Magnetite · Hybrid nanoparticles · Biomaterial

1 Introduction

Magnetic nanoparticles, Fe_3O_4, for example, have been extensively studied for application in biology and medicine due to their superparamagnetic behavior, high saturation magnetization, high magnetic susceptibility, and low biotoxicity [1, 2]. In order to overcome what is alleged to

This article is part of the Topical Collection on *Proceedings of the 16th Latin American Conference on the Applications of the Mössbauer Effect (LACAME 2018), 18-23 November 2018, Santiago de Chile, Chile*
Edited by Carmen Pizarro Arriagada

✉ Ângela Leão Andrade
angelala01@hotmail.com

✉ José Domingos Fabris

Extended author information available on the last page of the article

be some limiting characteristics of magnetite to be used for in vivo biological systems, as low colloidal stability, low circulation time in biological environments and eventually low affinity for target sites in the living body [3, 4], several nanohybrid systems magnetite-polymer have been reportedly developed or at least proposed [5].

The solvent displacement method, also known as nanoprecipitation, is certainly the simplest method to prepare nanodispersions of water-insoluble bioactive compounds systems. The method essentially consists of mixing an aqueous phase containing an emulsifier with a water-miscible organic solvent such as ethanol or acetone. The organic solvent may contain the dissolved bioactive compound, a polymer, and optionally oil and a lipophilic emulsifier. Empty (poly(L-co-D,L lactic acid-co-trimethylene carbonate (PLDLA-co-TMC)@(PEO-PPO-PEO) (poly(ethylene oxide)-poly(propylene oxide)-poly(ethylene oxide)) and hybrid nanoparticles ((poly(L-co-D,L lactic acid-co-trimethylene carbonate) (PLDLA-co-TMC)@PEO-PPO-PEO (poly(ethylene oxide)-poly(propylene oxide)-poly(ethylene oxide)@magnetite (Fe_3O_4)@tetramethylammonium hydroxide (TMAOH)) are promptly formed under the diffusion of the organic solvent into the aqueous phase, which induces interfacial nanodeposition of the bioactive compound at the interface between the organic and the aqueous phases [6, 7]. The polymer, which diffuses together with the organic solvent, is stranded at the interface and incorporates the bioactive compound. The emulsifier in the aqueous phase stabilizes and prevents the aggregation of the empty and hybrid nanoparticles. The organic solvent is then evaporated out from the nanodispersion under reduced pressure.

In this work, we coated TMAOH (tetramethylammonium hydroxide)-dispersed magnetite nanoparticles [8] with the poly(L-co-D,L lactic acid-co-trimethylene carbonate) polymer (or PLDLA-co-TMC, for short) through the solvent displacement method.

The main purposes of this research were: (i) to develop a new nanohybrid biomaterial based on Fe_3O_4/TMAOH/PLDLA-co-TMC through the solvent displacement method, and (ii) to compare some of its physical properties containing different amounts of the magnetite core.

2 Materials and methods

2.1 Reagents

Iron (III) chloride hexahydrate, $FeCl_3.6H_2O$ (Riedel-de Haen, France); sodium sulfite, Na_2SO_3 (Sigma-Aldrich, Japan); ammonium hydroxide, NH_4OH (Fluka, Germany); 25% aqueous tetramethylammonium hydroxide pentahydrate solution, $C_4H_{13}NO.5H_2O$ (TMAOH) (Aldrich, Germany, Japan), hydrochloric acid, HCl (Sigma-Aldrich). The PEO-PPO-PEO (poly(ethylene oxide)-poly(propylene oxide)-poly(ethylene oxide)) triblock copolymer (MW, 7680–9510) (Kolliphor® P188) was purchased from Sigma-Aldrich. Acetone (UN1090, ≤ 0.5% water) and methyl alcohol (UN1230, ≤ 0.10% water) were of HPLC grade from Tedia™ High Purity Solvents (Rio de Janeiro, Brazil). The poly (L-co-D,L lactic acid-co-trimethylene carbonate), or PLDLA-co-TMC:solvent corresponding to a volume ratio 70:30 was prepared as reported in ref. [9]. All chemicals were used as received.

2.2 Synthesis and functionalization of magnetite: Magnetic ferrofluid

Samples of Fe_3O_4 nanoparticles were obtained via the reduction-precipitation method, following the procedure described in details elsewhere [8, 10]. Essentially, the method consisted of adding 15 mL of 1 mol L^{-1} Na_2SO_3 to 22.5 mL of 2 mol L^{-1} $FeCl_3.6H_2O$ previously dissolved in

0.5 mol L^{-1} HCl, into a 1000 mL necked round bottom flask, while bubbling-in N_2 gas, in order to assure as much as possible a chemically inert atmosphere. Just after mixing Fe^{3+} and SO_3^{2-}, the color of the solution changed from light yellow to red and afterwards back to yellow. Meanwhile, 600 mL of a 0.5 mol L^{-1} ammonium hydroxide solution was quickly poured into the solution under vigorous stirring: a black precipitate was formed. The suspension containing the precipitate was centrifuged at 3000 rpm for 2 min; the supernatant was discarded. This procedure was repeated five times by redispersing the resultant cakes in distilled water. The obtained precipitate was labeled "mag". The magnetic nanoparticles were then treated for coating with tetramethylammonium hydroxide (TMAOH). Typically, 16 mL of commercial 25% TMAOH solution was added to the previously formed product and redispersed with a thin glass rod until obtaining homogeneous suspensions. 2 mL of this suspension was diluted tenfold in distilled water and the obtained ferrofluid was used for further coating with the polymer. Part of this suspension was then dried to obtain the final powders. The sample that was treated with TMAOH in order to obtain the surface coated magnetite nanoparticles was labeled "mag1".

2.3 Preparation of the hybrid nanoparticles

The solvent displacement method used to obtain the hybrid nanoparticles (Fe_3O_4/TMAOH/PLDLA-co-TMC) samples based on poly(L-co-D,L lactic acid-co-trimethylene carbonate) (PLDLA-co-TMC) was previously described [11, 12]. The aqueous or external phase (PEO-PPO-PEO, 37.5 mg, and Milliq water, 7.5 mL, with 0.25 mL, 0.50 mL and 1.00 mL of the diluted suspension of magnetite, meaning 2 mL of the suspension of magnetite tenfold diluted in distilled water) and the organic or internal phase (PLDLA-co-TMC, 20 mg, acetone, 2.2 mL, and methanol, 0.3 mL) were separately solubilized in ice-water bath under sonication (UP100H, hielscher - cycle 1, amplitude (%) 100) for one minute and two minutes, respectively. The colloidal solutions were maintained at room temperature. After, the organic phase was added dropwise (20 mL h^{-1} - Cole-Parmer®) into of the aqueous phase under sonication for three minutes. The colloidal solution was then rotoevaporated (IKA®HB10, Biovera) to remove the organic solvent (acetone and methanol); from this operation, only hybrid nanoparticles remained suspended in water. These resulting suspensions, which were correspondently labeled "mag1(0.25)", "mag1(0.5)" and "mag1(1.0)", were centrifuged (CS150FX, Hitachi) for 45 min at 18,000 rpm. The combination of the aqueous phase without the diluted suspension of magnetite (PEO-PPO-PEO, 37.5 mg, and Milliq water, 7.5 mL) with the organic phase (PLDLA-co-TMC, 20 mg, acetone, 2.2 mL, and methanol, 0.3 mL) was labeled "empty nanoparticles". The sedimented particles were repeatedly washed with doubly distilled water, acetone and methanol, before being frozen in liquid nitrogen and lyophilized for characterization.

2.4 Structural characterization techniques

The samples formed by an empty macromolecular cage of poly(L-co-D,L lactic acid-co-trimethylene carbonate) (PLDLA-co-TMC) only (which will be hereinafter referred to as simply "empty nanoparticles"), the hybrid nanoparticles (Fe_3O_4/TMAOH/PLDLA-co-TMC) and the TMAOH-dispersed (Fe_3O_4) magnetic nanoparticles were characterized by Fourier-transform infrared spectroscopy on an IRPrestige-21 Shimadzu® spectrometer, in which the FTIR spectrum was recorded in the range of 400–4000 cm^{-1}; the samples were homogenously dispersed in KBr at room temperature and pressed into discs. The powder X-ray diffraction patterns were obtained

with a Shimadzu XRD 6000 diffractometer, using Cu (Kα) radiation, with 2θ angles ranging from 29° to 70° at steps of 0.021° s^{-1}. The X-ray diffraction (XRD) data analysis was used to identify the crystalline components of the samples. Mössbauer spectra were collected at 298 K in a conventional transmission spectrometer in the constant acceleration mode and a $^{57}Co/Rh$ gamma-ray source with nominal activity of about 50 mCi, equipped with a transducer (CMTE model MA250) controlled by a linear function driving unit (CMTE model MR351). Values of Mössbauer isomer shifts are quoted relatively to an α-Fe foil at room temperature. The experimental data were fitted with Lorentzian functions by least-square fitting with WinNormos™ for Igor Pro™ software version 6.1. The magnetization measurements were made at room temperature (RT) on a LakeShore (model 7404) vibrating sample magnetometer (VSM).

3 Results and discussion

The infrared spectrum for PLDLA-co-TMC (Fig. 1a) showed bands at 1753 cm^{-1} (C = O stretching in the ester group), 1455 cm^{-1} (CH_3 bending), 1380 cm^{-1} (CH_2 wagging), 1266 and 1091 cm^{-1} (CO stretching), 1187 cm^{-1} (COC), at 792 cm^{-1} (CH) and at 753 cm^{-1} (-CH_2CH_2 - TMC) [13, 14].

The FTIR spectrum for the PEO-PPO-PEO (Fig. 1b) showed the characteristic bands of the surfactant at 1343 and 1110 cm^{-1}, which are due to the stretching of the O-H and C-O groups respectively [15–17].

The FTIR spectrum for the empty nanoparticle (Fig. 1c) showed signals assignable to PLDLA-co-TMC and to PEO-PPO-PEO. The non-displacement of the signals seems to indicate the lack of chemical interaction between the PLDLA-co-TMC and PEO-PPO-PEO in the empty nanoparticles.

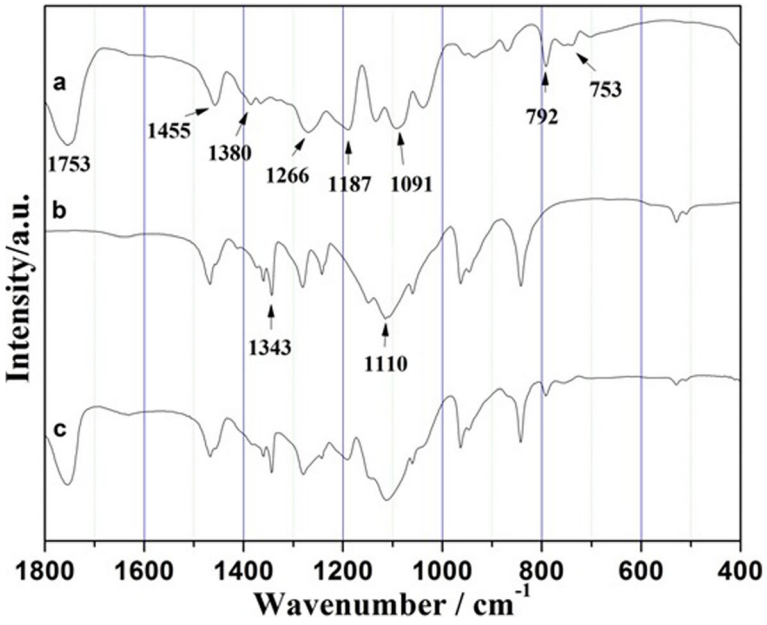

Fig. 1 Infrared spectra for the samples: a) PLDLA-co-TMC, b) PEO-PPO-PEO, and c) empty nanoparticle

The mag and mag1 samples (Fig. 2b, c) presented an absorption band centered at 581 cm^{-1} related to the molecular vibrations of Fe-O stretching [18]. From the infrared spectra of mag1, an absorption band at 977 cm^{-1} was assigned to the asymmetric (C-N) vibrational mode of TMAOH, which is generally observed in the 900–1000 cm^{-1} domain [8].

The FTIR spectra for the hybrid nanoparticles [mag1(0.25), mag1(0.5) and mag1(1.0)] evidenced that the Fe-O bands at 580 cm^{-1} are broadened and the intensity of the band at 977 cm^{-1} decreased. These samples also presented characteristic bands of the terpolymer (PLDLA-co-TMC). This suggests the occurrence of the terpolymer in hybrid nanoparticles [19], confirming the efficiency of the solvent displacement method to coat the TMAOH-dispersed magnetic nanoparticles. However, some bands associated with the C-O of the polymer sample (1116 cm^{-1} and 1280 cm^{-1}) are displaced in the hybrid samples (1110 cm^{-1} and 1255 cm^{-1}). Therefore, it is evident that there is an intermolecular interaction among the proton donor groups (-O and N) of mag1 and the proton acceptor groups (C-O) of the polymers [19]. Simultaneously, signals associated with the polymer at 842 cm^{-1} (C-H), 792 cm^{-1} (C-H) and 753 cm^{-1} ($-CH_2CH_2-$) decreased as the amount of magnetite increased in the hybrid nanoparticles. Considering that mag1(1.0) has the lowest coating mass and higher concentration of magnetite, the absence of the signal may indicate that the number of CH bonds available in the terpolymer has been reduced, to compensate the higher number of mag1 bonds.

Through the spectral characteristics of hybrid nanoparticles, it can be concluded that the terpolymer was chemically connected to the TMAOH-dispersed magnetic nanoparticles, creating functional hybrids of the PLDLA-co-TMC-magnetite.

Powder X-ray diffraction (XRD) patterns for the synthesized magnetic nanoparticles and TMAOH-dispersed magnetic nanoparticles incorporated in PLDLA-co-TMC, mag1(0.25), mag1(0.5) and mag1(1.0) are shown in the Fig. 3. It can be observed that the synthesized magnetic nanoparticles have crystalline structure with sharp reflection peaks at $2\theta = 30.0°$, 35.4°, 43.0°, 53.4°, 56.9° and 62.5°, corresponding to the diffraction of the crystal planes of

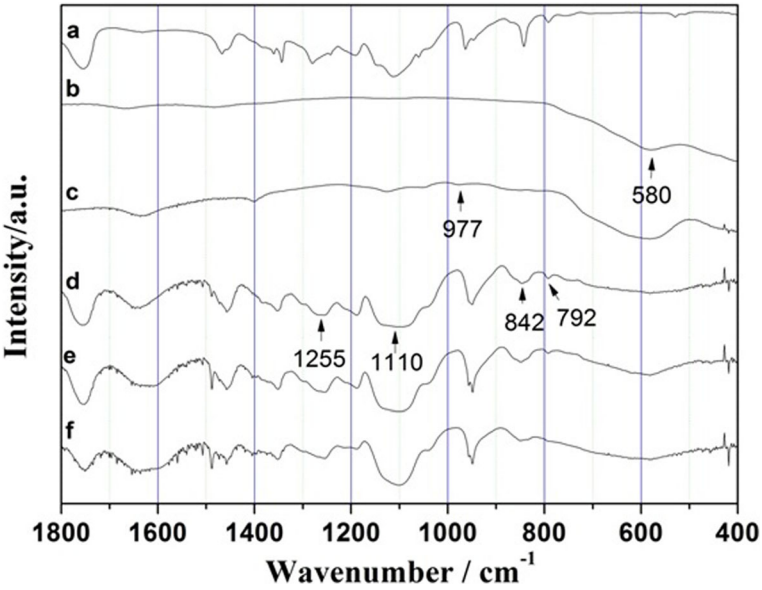

Fig. 2 Infrared spectra of the samples: **a**) empty nanoparticle, **b**) mag, **c**) mag1, **d**) mag1(0.25), **e**) mag1(0.5), and **f**) mag1(1.0)

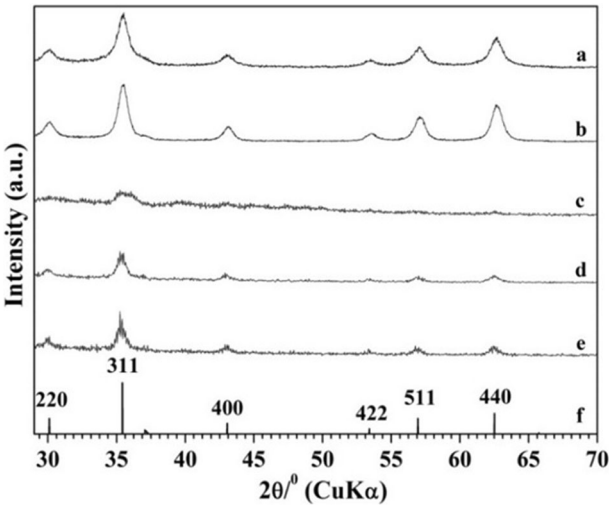

Fig. 3 X-ray diffraction patterns for the samples: **a**) mag, **b**) mag1, **c**) mag1(0.25), **d**) mag1(0.5), **e**) mag1(1.0), and **f**) magnetite (ICDD # 19–629)

magnetite 220, 311, 400, 422, 511 and 440, respectively (ICDD # 19–629). The XRD data for the copolymer composite with encapsulated Fe_3O_4 exhibits the same spinel peaks. As expected, the reflection peak intensities in these X-ray diffraction patterns for the mag1(0.25) sample are generally smaller than for the mag1(0.5) sample, which in turn are smaller than for the mag1(1.0) sample. This is explained by the fact that the sample mag1(0.25) contains a smaller amount of magnetite than the sample mag1(0.5), which in turn presents still a smaller amount than the sample mag1(1.0).

It was not observed any reflection peak due to another crystalline phase than magnetite.

The magnetization curves vs. applied magnetic field at 300 K for the mag sample just after its synthesis and also for the hybrid nanoparticles are shown in Fig. 4.

The polymer shell is non-magnetic shell and this explains that the lower M_s of hybrid nanoparticles of the mag sample. The saturation of magnetization depends on the volume fraction of magnetic nanoparticles and on the nature of their interactions within the polymer matrix.

The coercive force of mag sample is very low, or about 5 Oe, showing that this sample does not retain magnetization by removing the external magnetic field. The remanent magnetization of this same sample was nearly zero, and this indicated that there was almost no remaining magnetization by removing the external magnetic field. All these data, including of the coercive force and of the magnetic remanence, point that the mag sample behaves superparamagnetically, which favors its redispersion after the external magnetic field is removed. Because the mean particle size of these magnetic particles, as previously determined by scanning electron microscopy (for this same sample, ref. [10]), is about 10 nm, the dimension of each particle corresponds to a single crystal domain, exhibiting only one orientation of the giant magnetic moment. This is why the mag sample exhibited superparamagnetic properties. The particle sizes for the other samples, which are not superparamagnet, are larger (data not shown).

It is clear from the Table 1 that the saturation magnetization and the remanence magnetization values increase with the Fe_3O_4 content. This is due to the stronger inter-particle interaction within the whole sample matrix [20].

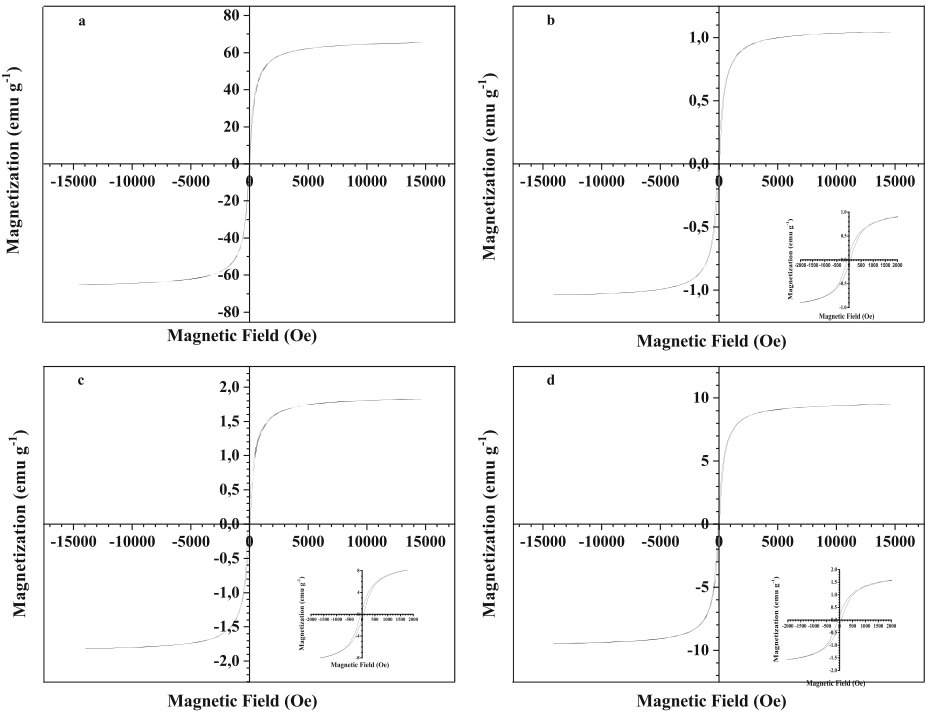

Fig. 4 Hysteresis loops for the samples **a**) mag, **b**) mag1(0.25), **c**) mag1(0.5), and **d**) mag1(1.0)

The Mössbauer spectrum for the sample mag at 298 K (Fig. 5; corresponding hyperfine parameters in the Table 2) consists of two sextets, one assignable to high spin Fe^{3+} on tetrahedral sites (B_{hf} = 48.04(3) T) and the other to mixed valence $Fe^{3+/2+}$ on octahedral sites (B_{hf} = 44.53(5) T) of the magnetite structure. Electron delocalization causes the nucleus to sense an averaged valence $Fe^{3+/2+}$. Considering that the recoilless fraction of octahedral sites at room temperature is 6% less than that of the tetrahedral sites [38] the relative area ratio RA_{oct}/RA_{tet} = 1.67 indicates that the magnetite obtained (mag sample) is fairly close to its pure stoichiometric form.

From Mössbauer data in relation to hybrid nanoparticles we can observe a decreasing values for the relative area ratio RA_{oct}/RA_{tet}, 1.53 for mag1(0.25), 1.47 mag1(0.5) and 1.40 mag1(1.0). This decrease indicates that the Fe^{2+} is being oxidized to Fe^{3+}. These results show that at higher Fe_3O_4 loadings, the difficulty of the encapsulation of Fe_3O_4 increased. Polymer coatings, for example, are known to favor the chemical protection of the magnetite preventing it from being degraded during or after the preparation of the hybrid system. Therefore, these results show that the amount of magnetite added for the sample mag1(1.0) was greater than the amount that the polymer can coat. The magnetite that has not been incorporated into the polymer should be partially oxidized.

Table 1 Magnetic parameters of the magnetic nanoparticle and nanocomposites (hybrid nanoparticles)

Sample	M_s/emu g^{-1}	H_c/Oe	M_r/emu g^{-1}
mag	67	5	0.01
mag1(0.25)	1.0	58	0.10
mag1(0.5)	1.7	60	0.16
mag1(1.0)	9.0	60	0.9

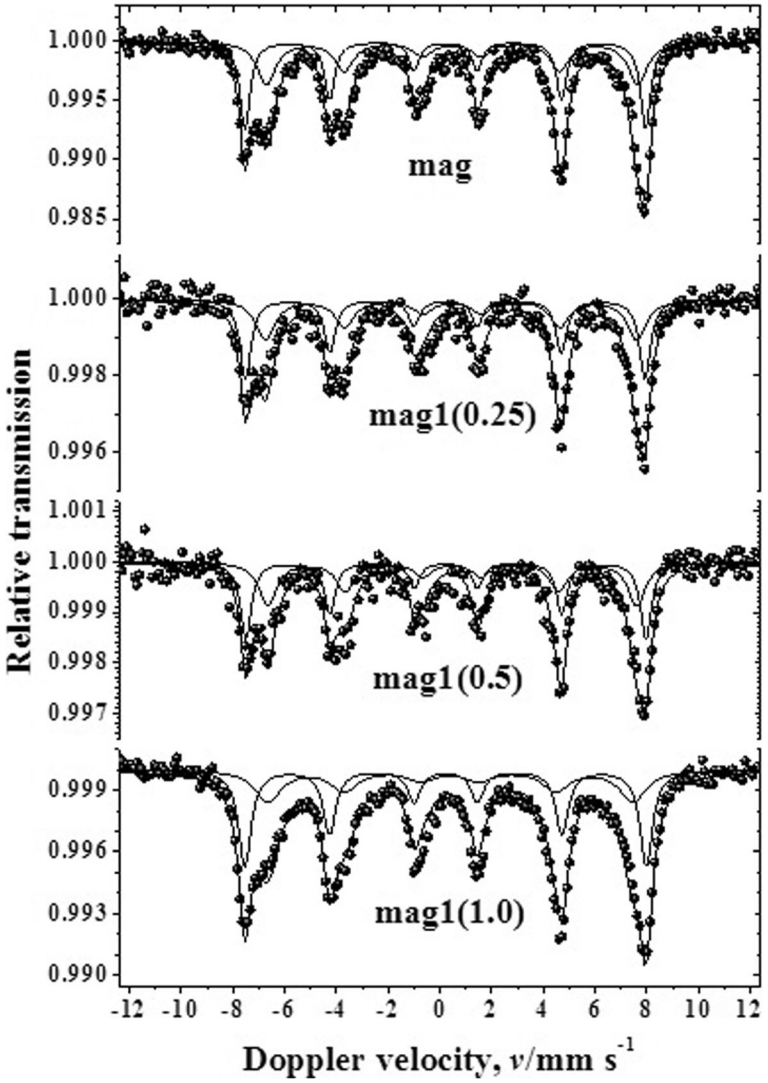

Fig 5 298 K-Mössbauer spectra for the samples: mag, mag1(0.25), mag1(0.50) and mag1(1.00)

4 Conclusions

A novel hybrid material based on nanoparticles of Fe_3O_4/TMAOH/PLDLA-co-TMC was prepared by the solvent displacement technique. The FTIR data provided enough insight to confirm the efficiency of the solvent displacement method to promote coating the TMAOH-dispersed magnetic nanoparticles with the terpolymer. The XRD data clearly point to a crystallographic order and a uniform arrangement of magnetic nanoparticles within the copolymer matrix. The vibrating sample magnetometry measurements indicate that at least part of the nanohybrids systems behaves superparamagnetically. The Mossbauer spectrum indicates that the obtained magnetite is fairly close to its pure stoichiometric form and that the maximum amount that can be encapsulated by the polymer occurred in sample mag1 (0.5). This magnetic

Table 2 Parameters from fitting ^{57}Fe Mössbauer spectra recorded at 298 K

Sample	^{57}Fe site		δ/mm s^{-1}	2ε/mm s^{-1}	Γ/mm s^{-1}	B_{hf}/T	RA/%
Mag	Fe_3O_4	[Fe^{3+}]	0.314(5)	−0.009(9)	0.47(2)	48.04(3)	37.4(1)
		{$Fe^{3+/2+}$}	0.569(8)	0.00(1)	0.87(3)	44.53(5)	62.6(1)
mag1(0.25)	Fe_3O_4	[Fe^{3+}]	0.31(1)	−0.01(2)	0.51(5)	47.89(8)	39.6(1)
		{$Fe^{3+/2+}$}	0.55(2)	−0.04(3)	0.88(6)	44.5(1)	60.4(1)
mag1(0.5)	Fe_3O_4	[Fe^{3+}]	0.33(1)	0.00(3)	0.50(4)	47.97(9)	40.5(1)
		{$Fe^{3+/2+}$}	0.57(2)	0.01(3)	0.81(6)	44.2(1)	59.5(1)
mag1(1.0)	Fe_3O_4	[Fe^{3+}]	0.323(3)	−0.005(7)	0.59(2)	48.14(3)	41.7(1)
		{$Fe^{3+/2+}$}	0.498(9)	0.01(2)	1.22(3)	43.8(1)	58.3(1)

δ = isomer shift relative to the αFe; 2ε = quadrupole shift; Γ = resonance line width; B_{hf} = magnetic hyperfine field; RA = relative subspectral area. [] denotes tetrahedral and {} octahedral symmetries of the Fe-O coordination sites of the spinel structure. [Fe^{3+}] and {$Fe^{3+/2+}$} stand, respectively, for iron in tetrahedral and octahedral coordination sites of the spinel structure of the magnetite. Numbers in parentheses are standard deviation over the last significant digit of the value, as output by the computer fitting program, based on the least squares algorithm

hybrid nanocomposite is revealed to be of real potential as drug carrier of therapeutical drugs destined to be locally delivered in live human tissues, under the thermal effect of magnetic hyperthermy, induced by an externally applied oscillating magnetic field. A nanosytem representing an initial step for further development of more advanced technology for medical practices in clinical therapy or even in diagnosis, in oncology.

Acknowledgements JD Fabris and LCD Cavalcante are indebted to the Brazilian National Council for the Scientific and Technological Development (CNPq), for the financial support under the grants # 304958-2017-4 and # 313431/2017-5, respectively. The Brazilian Coordination for the Improvement of Higher Education Personnel (CAPES) granted a DSc studenship to VO Machado at Military Insitute of Engineering (Brazil).

References

1. Dresco, P.A., Zaitse, V.S., Gambino, R.J., Chu, B.: Preparation and properties of magnetite and polymer magnetite nanoparticles. Langmuir. **15**(6), 1945–1951 (1999). https://doi.org/10.1021/la980971g
2. Tartaj, P., Morales, M.D., Veintemillas-Verdaguer, S., Gonzalez-Carreno, T., Serna, C.J.: The preparation of magnetic nanoparticles for applications in biomedicine. J. Phys. D. Appl. Phys. **36**(13), R182–R197 (2003). https://doi.org/10.1007/978-1-4939-6840-4_5
3. Mornet, S., Vasseur, S., Grasset, F., Duguet, E.: Magnetic nanoparticle design for medical diagnosis and therapy. J. Mater. Chem. **14**(14), 2161–2175 (2004). https://doi.org/10.1039/B402025A
4. Crucho, C.I.C., Barros, M.T.: Polymeric nanoparticles: a study on the preparation variables and characterization methods. Mater. Sci. Eng. C. **80**, 771–784 (2017). https://doi.org/10.1016/j.msec.2017.06.004
5. Khalkhali, M., Rostamizadeh, K., Sadighian, S., Khoeini, F., Naghibi, M., Hamidi, M.: The impact of polymer coatings on magnetite nanoparticles performance as MRI contrast agents: a comparative study. DARU J. Pharm. Sci. **23**(45), (2015). https://doi.org/10.1186/s40199-015-0124-7
6. Quintanar-Guerrero, D., Allemann, E., Fessi, H., Doelker, E.: Preparation techniques and mechanisms of formation of biodegradable nanoparticles from preformed polymers. Drug Dev. Ind. Pharm. **24**(12), 1113–1128 (1998). https://doi.org/10.3109/03639049809108571
7. Couvreur, P., Barratt, G., Fattal, E., Legrand, P., Vauthier, C.: Nanocapsule technology: a review. Crit. Rev. Ther. Drug Carrier Syst. **19**(2), 99–134 (2002). https://doi.org/10.1615/CritRevTherDrugCarrierSyst.v19.i2.10
8. Andrade, A.L., Fabris, J.D., Ardisson, J.D., Valente, M.A., Ferreira, J.M.F.: Effect of tetramethylammonium hydroxide on nucleation, surface modification and growth of magnetic nanoparticles. J. Nanomater. Article ID 454759. 10 (2012). https://doi.org/10.1155/2012/454759
9. Motta, A.C., Duek, E.A.R.: Synthesis and characterization of a novel terpolymer based on L-lactide, D,L-lactide and trimethylene carbonate. Mater. Res. **17**(3), 619–626 (2014). https://doi.org/10.1590/S1516-14392014005000067

10. Andrade, A.L., Souza, D.M., Pereira, M.C., Fabris, J.D., Domingues, R.Z.: Magnetic properties of nanoparticles obtained by different chemical routes. J. Nanosci. Nanotechnol. **9**(3), 2081–2087 (2009). https://doi.org/10.1166/jnn.2009.423
11. Barichello, J.M., Morishita, M., Takayama, K., Nagai, T.: Encapsulation of hydrophilic and lipophilic drugs in PLGA nanoparticles by the nanoprecipitation method. Drug Dev. Ind. Pharm. **25**(4), 471–476 (1999). https://doi.org/10.1081/DDC-100102197
12. Fessi, H., Puisieux, F., Devissaguet, J.P., Ammoury, N., Benita, S.: Nanocapsule formation by interfacial polymer deposition following solvent displacement. Int. J. Pharm. **55**(1), R1–R4 (1989). https://doi.org/10.1016/0378-5173(89)90281-0
13. Mas, B.A., Cattani, S.M.M., Rangel, R.C.C., Ribeiro, G.A., Cruz, N.C., Leite, F.L., Nascente, P.A.P., Duek, E.A.R.: Surface characterization and osteoblast-like cells culture on collagen modified PLDLA scaffolds. Mater. Res. **17**(6), 1523–1534 (2014). https://doi.org/10.1590/1516-1439.269414
14. Motta, A.C., Duek, E.A.R.: Synthesis and characterization of the copolymer poly(L-co-D,L lactic acid). Polim.: Cienc. Tecnol. **17**(2), 123–129 (2007). https://doi.org/10.1590/S0104-14282007000200011
15. Fousteris, E., Tarantili, P.A., Karavas, E., Bikiaris, D.: Poly(vinyl pyrrolidone)-poloxamer-188 solid dispersions prepared by hot melt extrusion. J. Therm. Anal. Calorim. **113**(3), 1037–1047 (2013). https://doi.org/10.1007/s10973-012-2885-2
16. Vyas, V., Sancheti, P., Karekar, P., Shah, M., Pore, Y.: Physicochemical characterization of solid dispersion systems of tadalafil with poloxamer 407. Acta Pharma. **59**(4), 453–461 (2009). https://doi.org/10.2478/v10007-009-0037-4
17. Saritha, A., Shastri, N.: Preparation, physico chemical characterization of solid dispersions of tenoxicam with poloxamer. J. Pharm. Sci. Technol. **2**(9), 308–311 (2010)
18. Wei, Y., Han, B., Hu, X., Lin, Y., Wang, X., Deng, X.: Synthesis of Fe_3O_4 nanoparticles and their magnetic properties. Chin. Mater. Conf. **27**, 632–637 (2012). https://doi.org/10.1016/j.proeng.2011.12.498
19. Komatsu, D., Mistura, D.V., Motta, A., Domingues, J.A., Hausen, M.A., Duek, E.: Development of a membrane of poly (L-co-D,L lactic acid-co-trimethylene carbonate) with aloe vera: an alternative biomaterial designed to improve skin healing. J. Biomater. Appl. **32**(3), 311–320 (2017). https://doi.org/10.1177/0885328217719854
20. Jayakrishnan, P., Ramesan, M.T.: Studies on the effect of magnetite nanoparticles on magnetic, mechanical, thermal, temperature dependent electrical resistivity and DC conductivity modeling of poly (vinyl alcohol-co-acrylic acid)/Fe_3O_4 nanocomposites. Mater. Chem. Phys. **186**, 513–522 (2017). https://doi.org/10.1016/j.matchemphys.2016.11.028

Affiliations

Vagner de Oliveira Machado[1] · Ângela Leão Andrade[2] · Luis Carlos Duarte Cavalcante[3,4] · José Domingos Fabris[4,5] · Rosana Zacarias Domingues[4] · José Domingos Ardisson[6] · Luís E. Fernandez-Outon[6] · Carmen Pizarro[7] · Carlos Nelson Elias[1]

1 Laboratory of Biomaterials, Military Institute of Engineering (IME), Rio de Janeiro, RJ 22290-270, Brazil

2 Department of Chemistry, Federal University of Ouro Preto (UFOP), Ouro Preto, MG 35400-000, Brazil

3 Center of Natural Sciences, Federal University of Piauí (UFPI), Teresina, PI 64049-550, Brazil

4 Department of Chemistry, Federal University of Minas Gerais (UFMG), Belo Horizonte, MG 31270-901, Brazil

5 Institute of Chemistry, Federal University of Uberlândia (UFU), Uberlândia, MG 38400-902, Brazil

6 Laboratory of Applied Physics, Center for the Development of the Nuclear Tecnology (CDTN), Belo Horizonte, MG 31270-901, Brazil

7 Faculty of Chemistry and Biology, University of Santiago, Chile (USACH), Santiago, Chile